Alexandria Engineering Journal (2022) 61, 5033–5050

HOSTED BY

Alexandria University

Alexandria Engineering Journal

www.elsevier.com/locate/aej
www.sciencedirect.com

4 E's (Energy, Exergy, Economic, Environmental) performance analysis of air heat exchanger equipped with various twisted turbulator inserts utilizing ternary hybrid nanofluids

Vikash Kumar, Rashmi Rekha Sahoo *

Department of Mechanical Engineering, Indian Institute of Technology (BHU), Varanasi 221005, India

Received 24 April 2021; revised 10 August 2021; accepted 12 September 2021
Available online 15 December 2021

KEYWORDS

THNF;
PEC;
SI;
Irreversibility;
Entropy;
Wavy fin;
Turbulators;
Exergy;
DTTI;
PTTI;
TTI;
HX

Abstract Advancement in technologies needs a critical heat removal technique for better exergo-economic performance of compact air heat exchangers. The passive technique is used for heat transfer improvement with various turbulators inserts TTI, PTTI, and DTTI in plain tube air heat exchanger. This paper investigates the exergo-economic sustainable performance of heat exchanger devices assisted with water-based different tripartite hybrid nanofluids under various geometrical turbulator inserts modifications. Simulation is proceeded for tripartite hybrid nanofluids of mainly six various compositions based on the nanoparticles morphology variant and three different turbulators inserts at the core of plain tubes heat exchanger. The four E's (Exergy, Energy, Economic, and Environmental) aspects with sustainability analysis of the device are studied with operating parameters. Results revealed that only nanofluid would not be useful for energy enhancement, while turbulator inserts with THNF result in a significant improvement in the thermohydraulic performance of the device. The device inserts with DTTI in plain tubes using THNF 6 results in the highest26% overall heat transfer coefficient, 2.94% exergy efficiency, 5.04% performance index, and higher sustainability index at low Reynolds number, meanwhile turbulator inserts yield to highest 91.94% operating cost and equivalent CO_2emissions. DTTI with THNF 6 is preferred as working fluid as PEC ranges highest 1.42–2.35, and THNF 2 working fluid should be least preferred due to its high operating cost.

1. Introduction

Heat exchangers have been widely used in the automotive industry, industrial applications, and processes. Modified technologies have increased thermal loads in a compact heat

* Corresponding author.
E-mail address: rrsahoo.mec@itbhu.ac.in (R.R. Sahoo).
Peer review under responsibility of Faculty of Engineering, Alexandria University.

https://doi.org/10.1016/j.aej.2021.09.037

Nomenclature

$\dot{m}$	Mass flow rate
Q	Heat transfer (W)
A_a	Air side surface area
A_a	Total surface area
A_f	Fluid surface area
A_{fin}	Fin surface area
A_{fr}	Frontal area of HX
Al_2O_3	aluminium oxide
C_p	Specific heat (J/kg. K)
CuO	copper oxide
D_h	Hydraulic diameter (mm)
f_f	friction factor
h	Heat transfer coefficient (W/m^2. K)
Nu	Nusselt number
p	Pressure (Pa)
P_d	Dimpled pitch
P_l	Longitudinal tube pitch
P_p	Perforated pitch
P_t	Transverse tube pitch
Re	Reynolds number
T	Temperature (°C)
TiO_2	Titanium oxide
Y	Twisted pitch
α	Thermal conductivity (W/m. K)

Greek symbols

τ	Dynamic viscosity (Pa. s)
ρ	Density (kg/m^3)
ω	volume fraction
ζ	Shape coefficient

Abbreviation

CF	Colburn factor
CFR	Coolant flow rate
DTTI	Dimpled twisted turbulator insert
HX	Heat exchanger
MWCNT	Multi-walled carbon nanotube
PEC	Performance evaluation criteria
PT	Plain tube
PTTI	Perforated twisted turbulator insert
SI	Sustainability index
THNF	Tripartite hybrid nanofluid
TTI	Twisted Turbulator insert

Subscripts

a	*air*
p	pump
pp	Pumping power
pf	primary fluid
eff	effective
f	fluid
i	inlet
e	exit
max	maximum
gen	Generation
o	Dead state
np	nanoparticles
ce	Coolant exit
hnf	Hybrid nanofluid
nf	Nanofluid

exchanger and therefore heat transfer improvement techniques have a focus on thermofluid research to establish an energy-efficient heat exchanger (HX) [1] and avoids thermal failure of the HX. Heat transfer improvement technique has broadly classified into two categories mainly active and passive. The active technique requires an external power agent like a magnetic field, vibration while the latter technique does not require any external power source and only utilizes the flow energy for heat transfer augmentation. The passive method includes the use of fin addition, geometrical modification, tube inserts, and others while its easy installation at a lower cost makes it superior and widely used [2]. Twisted tape and helically coiled inserts are widely used as passive heat transfer techniques as these inserts improve heat transfer effectiveness, swirl flow generation, flow continuation, elongated residence time and generates a secondary flow in a direction perpendicular to the flow [3-5]. Several studies have been studied to intensify heat transfer performance using twisted turbulator insert [TTI] along with little geometrical modification. In the following, some recent studies on turbulators will be reviewed. Eiamsa-ardet al. [6] analyzed heat transfer and thermohydraulic performance of peripheral v-cut twisted turbulator inserts and compared them to the plain tube (PT). The author revealed TTI augmented heat transfer on increased depth ratio and decreased width ratio of v-cut. Murugesan et al. [7-9] investigated a cumulative impact on nusselt number and friction factor on introducing twisted turbulators of peripherally v-cut configuration, rectangular-cut configuration, and trapezoidal cut TTs. The author revealed that peripheral cut enhanced fluid mixing and thus improves heat transfer performance. Chu et al [10] later investigated TTI in a heat exchanger obtained an enhanced nusselt number and friction factor and successfully achieved the performance evaluation criteria (overall performance index) in the range of 1.18 to 1.23. Nakchi et al. [11,12] investigated HXs with double cut and rectangular cut TTs. The authors concluded a net enhancement in the Nusselt number index in the range of 2.3–2.9 ata penalty in pressure index of 1.4–1.8. Some researchers introduced novel perforated Twisted turbulators inserts (PTTI) of various perforates for further heat transfer improvement. Like Suri et al. [13] introduced squares centered perforated twisted turbulators and compared to the TTI and revealed that due to the presence of multiple squared perforates in the TTI a further higher heat transfer and friction factor achieved in the HX as perforated shape provides swirl induction, fluid mixing, and secondary flows. While Nananet al. [14] introduced perforated helical twisted turbulators and revealed a net decrement in heat transfer and frictional penalty compared to helically twisted turbulators. Most researchers [4,15,16] used PTTI to study thermohydraulic characteristics of HX and revealed an enhancement in heat transfer and friction factor compared to PT. Also, researchers focused on some other geometrical alter-

ations in Twisted turbulators like heat transfer effects due to the presence of delta winglets [17]. Eiamsa-ardet al. [18] reported a net performance enhancement of 13% compared to TTI when delta winglets were introduced at periphery while on further another study [19] when delta winglets introduced at center caused a net performance enhancement 40% higher than TTI. Also, geometrical modification dimple twisted turbulator inserts (DTTI) enhanced the heat transfer performance. Ligraniet al. [20] introduced three different pitch lengths of a circular centered dimple in TTI and revealed a net performance evaluation index of 1.6 at a lower dimpled pitch ratio author also claimed that due to the presence of dimpled curvature turbulent intensity caused an increase in the speed and also dimpled curvature helps to induce vortices in fluid flow causes a heat transfer augmentation. In Passive techniques, the utilization of nanofluid rather than a conventional fluid is another option for thermal performance improvement in HXs. Several authors utilized nanofluid as a working fluid in different engineering applications such as refrigeration application [21], solar energy-based application [22,23], electronic cooling systems [24,25], heat exchangers [26,27], natural circulation loop [28], and automotive industry [29,30]. Nanofluid is a better heat transfer agent compared to ordinary fluid thus makes it suitable to be used in various applications. Better thermal enhancement is achieved in presence of nanofluid due to the combined effect of various mechanisms, like nanoparticle interaction and clustering for enhanced thermal conductivity, Brownian motion of the particles in fluid flow, interfacial fluid–solid particle layering, nanoparticle shape factor [31].Anwar et al. [32,33] investigated the influence of the shape effect and shape factor of nanoparticles on the heat transfer mechanism and concluded a net thermal enhancement of 9.5%.Several studies [34,35] revealed nanoparticle addition to the primary fluid enhances the heat-carrying capacity and plays a crucial role to be selected as working fluid in HXs.Sh eikholeslamiet al. [36] numerically investigated the heat transfer behavior of nanomaterial with modified helical turbulator and obtained a reduction in thermal irreversibility of 89.95% with increased pumping power.Although TTI was also investigated in a wavy tube of different turbulator tapes by Hasanpouret al. [37]. The author revealed that HX outcomes higher Nusselt number and friction factor compared to simple tape except for porous media which has lesser friction factor. Esmaelzadehet al. [38] investigated thermo-hydraulic performance of HX using nanofluid of various tape thicknesses. They found 34.5% higher heat transfer using nanofluid with larger tape thickness comparatively. Various nanofluids like Al_2O_3-water [39], TiO_2–SiO_2 –water [40], TiO_2-water [41], CuO-water [42] was investigated with twisted tapes and resulted in a better heat transfer medium. Therefore, combined nanofluid and turbulators improve HX performance. As per the literature review, various nanofluids of different types have been studied, at low concentration yields excellent heat transfer agent. Recently researchers [43-46] focused on a new type of nanofluid Tri/Ternary/Tripartite hybrid nanofluid [THNF] which at lower volume concentrations yields a better overall performance index in HXs like evaporative coolers, automotive radiator applications. Although thermal devices generate irreversibility which is also a significant parameter to analyze a thermal system to identify the exergy distribution. Bahiaei et al. [47] studied efficiency and entropy generation on an electronic cooling HX using hybrid nanofluid compounded graphene –silver nanoparticles. The author claimed nanofluid remarkably reduces the overall temperature. Bahiraeiet al. [48] investigated a double pipe HX with Twisted turbulators and revealed a net lower entropy generation in cross arrangement than a parallel arrangement of turbulators. Eiamsa-ard et al. [49] investigated a DTTI with TiO2-water as a nanofluid and revealed that a lower pitch and lower nanoparticle concentration yields a better HX. Also, Singh et al. [50] performed an experimental investigation on TTI using a hybrid nanofluid composed of Al_2O_3-TiO_2/ water and obtained enhanced overall performance. Meanwhile, several studies are available that analyzethe second law of thermodynamics for nanofluids [51-53]. Turbulator inserts offerfluid flow destruction and boundary layer regeneration causes enhanced heat transfer, which is a motivation to select turbulators. From the literature review, no research study is availableon four E's analysis using THNF's as a working fluid to the turbulator inserts in air HX as well as no study available for the suitable selection of THNF as a working fluid to be utilized in a compact heat exchanger. The present investigation deals with four E's (Energy, Exergy, Economic, and Environmental) comparative analysis of air heat exchangersusing THNF's as working fluid utilizing various Turbulators. The novelty of the present investigation are:-

- Four E's analysis of six different THNF utilizes as a hot working fluid in tube sideof a compact airHX.
- Effect of turbulator inserts (TTI, PTTI, and DTTI) in air HX with THNF as working fluid on the Four E's.
- The combined effect of THNF's and turbulators inserts on thermohydraulic parameters [Performance Evaluation Criteria, Sustainability index, Performance Index and Second law analysis] of air HX.
- CO_2discharge and running cost analysis for sagacious selection of turbulators and THNF's.

2. Modeling and simulation

The theoretical performance-based analysis was studied on a wavy fin and staggered tube air heat exchanger, cross unmixed fluid flow type, with some dimensional detail and fluid flow directions as shown in Fig. 1. Air passes through the fin gap and hot fluid passes through staggered tubes. Meanwhile, a detailed dimension of the HX on both sides, air, and hot fluid sideare measured in the laboratory and tabulated in Table 1. Also, geometrical modifications inserts of TTI, PTTI, and DTTI within tubes with dimensional details studied have shown in Fig. 2 and tabulated in Table 2.The present analysis focuses on exergy, energy-economic, and environmental analysis, with performance evaluation of an air HX of staggered tube arrangement using different THNFs comprised of three different nanoparticles in terms of properties, behavior, and shape. Also, the further investigation focuses on the effect of various inserts [TTI, PTTI, DTTI] in air heat exchanger on second law analysis with parameters entropy generation, irreversibility, and second law efficiency with Reynold number as varying parameter. For analysis, the following general assumptions are stated below.

- Heat rejected from THNF isgained by air (No heat loss to the environment)

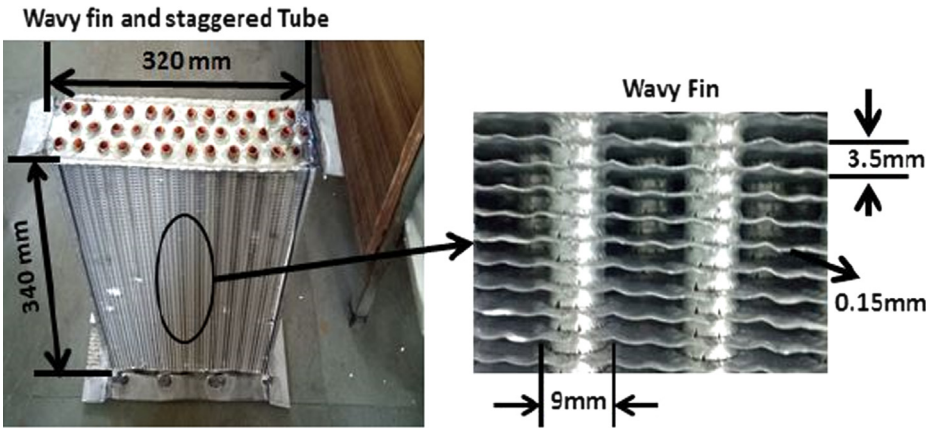

Fig. 1 Unmixed cross fluid flow Air Heat Exchanger.

Table 1 Dimensional details of selected compact Air heat Exchanger.

Description	Air Side	Coolant side
Fin side pitch (mm)	3.5	
Fin thickness (mm)	0.15	
Tube outer diameter (mm)		9
Tube thickness (mm)		0.5
Longitudinal Pitch (mm)	19.6	
Transverse Pitch (mm)	24.8	
Depth of HX(D) (mm)	54	
Tube Arrangement		Staggered
Free flow area/Frontal area	0.79	0.128
Fin area/Total Area	0.83	

- The compact HX device operated at a steady-state steady flow.
- Flow is a fully developed flow.
- The thermophysical properties of a fluid determine at mean temperature.
- Inserts resistance is ignored.

2.1. Numerical model in airside analysis

Air heat exchanger analysis, airside Colburn factor, Wang et al. [54] proposed a correlation to determine Colburn factor of HX with wavy fin and staggered tube configuration is determined as:

$$CF = \frac{1.201}{ln\left(Re_a^{2.921}\right)}. \tag{1}$$

Reynolds Number and mass velocity on airside is determined as,

$$MV_a = \frac{m_a}{A_{fr}} \text{and} Re_a = MV_a * \frac{D_a}{\mu_a}. \tag{2}$$

Convective heat transfer coefficient on airside is evaluated as,

$$h_a = \frac{CF * MV_a * cp_a}{Pr_a^{2/3}}. \tag{3}$$

Fin efficiency of wavy configuration has determined as,

$$\eta_{fin} = \frac{tanh\left(mr\acute{E}\mu\right)}{mr\acute{E}\mu}.$$

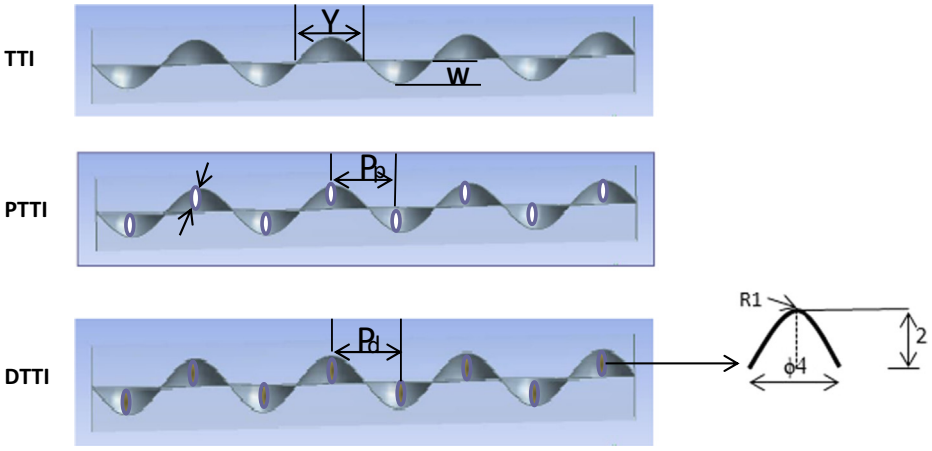

Fig. 2 Dimensional and pictorial configuration of modified Turbulataors inserts (TTI, PTTI, and DTTI).

Table 2 Detail dimensions of studied Turbulator inserts.

Turbulators	Y [mm]	W [mm]	Y/W	P_p [mm]	P_d [mm]	P_p/Y	P_d/Y	$Insertst_i$ Thickness [mm]
TTI	85	5	17	____	____	___	___	0.5
PTTI	85	5	17	21	____	0.25	____	0.5
DTTI	85	5	17	____	21	____	0.25	0.5

Where non-dimensional parameter and geometrical parameters that influence fin efficiency is determined as,

$$\kappa = \left(\frac{R_{eq}}{r} - 1\right) * \left(1 + 0.35\left(ln\frac{R_{eq}}{r}\right)\right). \tag{5}$$

$$\frac{R_{eq}}{r} = 1.27 * \left(\frac{Y_l}{Y_m} - 0.3\right)^{0.5}. \tag{6}$$

$$Y_m = \frac{P_l}{2} \text{and} Y_l = \sqrt{\left(\frac{P_t}{2}\right)^2 + \left(\frac{P_l}{2}\right)^2}. \tag{7}$$

Heat capacity of air is evaluated as,

$$C_a = \rho_a * V_a * A_{fr} * cp_a. \tag{8}$$

2.2. Thermophysical properties of tripartite hybrid nanofluids [Hot Fluid]

The tri hybrid nanofluid composition consists of three various nanoparticles (based on shape, nature, characteristics) well spread mixed in the primary fluid water. Heat exchanger performance depends upon the thermophysical properties of the working fluid. Therefore, density, specific heat capacity, thermal conductivity, and viscosity play a key role in heat transfer and pressure drop penalty in a heat exchanger. Thus it is an essential task to predict the thermophysical properties accurately. To investigate the application of nanofluid in a heat exchanger, following amalgamations of ternary nanoparticles were mixed, 0.6% of total volume concentration into the primary fluid water:

i. Al_2O_3 + CuO + TiO_2
ii. Al_2O_3 + CuO + Graphene
iii. Al_2O_3 + CuO + MWCNT
iv. Al_2O_3 + TiO_2 + Graphene
v. Al_2O_3 + TiO_2 + MWCNT
vi. Al_2O_3 + Graphene + MWCNT

Detail thermophysical characteristics of selected nanoparticles are listed in Table 3. The density of the tripartite hybrid nanofluid is calculated as [44]:

$$\rho_{hnf} = \omega_1\rho_1 + \omega_2\rho_2 + \omega_3\rho_3 + (1 - \omega_1 - \omega_2 - \omega_3)\rho_{pf}. \tag{9}$$

Subscripts 1, 2, and 3 represent the three different nanoparticles of an individual composition tripartite hybrid nanofluid where $\omega = \omega_1 + \omega_2 + \omega_3$ which represents the total volume fraction. Tripartite hybrid nanofluid heat capacity is expressed as [55]:

$$\left(\rho c_p\right)_{hnf} = \omega_1\left(\rho c_p\right)_1 + \omega_2\left(\rho c_p\right)_2 + \omega_3\left(\rho c_p\right)_3 + (1 - \omega_1 - \omega_2 - \omega_3)\left(\rho c_p\right)_{pf}. \tag{10}$$

Transport fluid properties of the tripartite hybrid nanofluid depend upon the primary fluid, nanoparticle morphology (spherical, platelet, and cylindrical), nanoparticle type, and individual volume concentration of nanoparticle. Thus, Effective dynamic viscosity and effective thermal conductivity of tripartite hybrid nanofluid are evaluated as [56]:

$$\omega\tau_{hnf} = \omega_1\tau_{nf,1} + \omega_2\tau_{nf,2} + \omega_3\tau_{nf,3}. \tag{11}$$

$$\omega\alpha_{hnf} = \omega_1\alpha_{nf,1} + \omega_2\alpha_{nf,2} + \omega_3\alpha_{nf,3}. \tag{12}$$

Where, $\tau_{nf,i}$ and $\alpha_{nf,i}$ are dynamic viscosity and thermal conductivity, respectively, for the mono nanofluid for total volume fraction consisting of i^{th}(i = 1, 2, or 3) kind of suspended nanoparticle into the base fluid. Nanofluid viscosity and conductivity of the i^{th} kind of nanoparticle (of required shape) spread are determined respectively,

$$\tau_{nf,i} = \tau_{pf}\left(1 + \beta_i\omega + \lambda_i\omega^2\right) \tag{13}$$

$$\frac{\alpha_{nf,i}}{\alpha_{pf}} = \frac{\alpha_{p,i} + (\zeta_i - 1)\alpha_{pf} + (\zeta_i - 1)\omega\left(\alpha_{p,i} - \alpha_{pf}\right)}{\alpha_{p,i} + (\zeta_i - 1)\alpha_{pf} - \omega\left(\alpha_{p,i} - \alpha_{pf}\right)} \tag{14}$$

Where the enhancement coefficients for the dynamic viscosity (β and λ) and empirical shape coefficient, ζ, for different shapes of nanoparticles are enlisted in Table 4. Different shapes and sizes of the nanoparticle influence its thermophysical properties. MWCNT (Multi-Walled Carbon Nanotube) nanoparticles are cylindrical, while, graphene nanoparticles are of platelet shape meanwhile remaining nanoparticles are of spherical morphology. Above empirical correlations were used in the entire investigation to determine the thermophysical properties of Tripartite hybrid nanofluids.

2.3. Heat exchanger performance evaluation

Hot side total heat capacity rate is given by,

$$C_f = \rho_{hnf}V_f c_{p,hnf}. \tag{15}$$

Hot fluid passes through tubes and under steady flow parallel tube combination pressure drop in a single tube is expressed as,

$$\Delta p_f = 0.5 \times f_f \times \frac{L}{D_h} \times \rho_{hnf} \times V^2. \tag{16}$$

Where Nusselt number and friction factor for plain tube fluid flow under turbulent flow regime has determined using suitable correlations proposed by Gnielinski [57];

$$f_f = \left[1.58 \times \ln(Re_f) - 3.28\right]^{-2}, 0.5 < pr_f < 2000, 3000 < Re_f < 5000000. \tag{17}$$

Table 3 Nanoparticles thermophysical characteristics [27,43]

Particles	Density (kg/m^3)	Specific heat (J/kg.K)	Thermal conductivity (W/mK)	Particle Size (nm)	Morphology
Aluminium Oxide (Al_2O_3)	3890	880	40	50	Spherical
Copper Oxide (CuO)	6310	531	18	50	Spherical
Titanium Oxide (TiO_2)	4170	711	4.8	40	Spherical
Graphene	2200	790	5000	50	Platelets
MWCNT	2100	740	3007.4	40	Cylindrical

Table 4 Enhancement and empirical morphology coefficients.

Morphology	Spherical	Platelet	Cylindrical
β	2.5	37.1	13.5
λ	6.2	612.6	904.4
ζ	3	5.7	4.9

$$Nu = \left[(Re_f - 1000) \times \mathrm{Pr}_f \times 0.5 \times \left(\frac{f_f}{1 + 12.7 \times \left(\mathrm{Pr}_f^{2/3} - 1 \right) \times \left(\frac{f_f}{2} \right)^{0.5}} \right) \right]. \tag{18}$$

Where non-dimensional parameters evaluated as, $\mathrm{Pr}_f = \frac{\tau_{hnf} C_{p,hnf}}{\alpha_{hnf}}$ and $Re_f = \frac{\rho_{hnf} V D_h}{\tau_{hnf}}$.

Now, under the passive technique when Twisted turbulator inserts introduced, Nusselt number in turbulent flow has determined a correlation proposed by Mangliket al. [58]

$$Nu_{TTI} = 0.023 Re_f^{0.8} \mathrm{Pr}_f^{0.4} \left(1 + 0.769 \frac{2D_h}{Y} \right) \left(\frac{\pi}{\pi - 4t_i D_h} \right)^{0.8} \left(\frac{\pi + 2 - 2t_i D_h}{\pi - 4t_i D_h} \right)^{0.2} \tag{19}$$

While friction factor for twisted turbulator inserts has been determined using correlation of Smithberg and Landis proposed for a turbulent case with water as fluid flow [59] as,

$$f_f = 4 \left(0.046 + 2.1 \left(\frac{Y}{D_h} - 0.5 \right)^{-1.2} \right) \left(\frac{Re_f}{1 + 2/\pi} \right)^{-Z} \tag{20}$$

Where,

$$Z = 0.2 \left(1 + 1.7 \left(\frac{Y}{D_h} \right)^{-0.5} \right) \tag{21}$$

While moving to the next turbulator, PTTI and DTTI, friction factor and Nusselt number has been determined using correlation proposed by Dagdevir and Ozeceyhan [60] respectively;

For Perforated Twisted Turbulator inserts case,

$$f_f = 0.986776 Re_f^{-0.28012} \left(0.01 + \frac{P_p}{Y} \right)^{-0.13672}, 2 < \mathrm{Pr}_f < 36.2, 2300 < Re_f < 22754. \tag{22}$$

$$Nu_{PTTI} = 0.034299 Re_f^{0.785361} \mathrm{Pr}_f^{0.413538} \left(0.01 + P_p Y \right)^{-0.09157}. \tag{23}$$

When Dimpled twisted turbulator inserts case [59],

$$f_f = 0.970112 Re_f^{-0.27091} \left(0.01 + \frac{P_d}{Y} \right)^{-0.13672}, 2 < \mathrm{Pr}_f < 36.2, 2300 < Re_f < 22754. \tag{24}$$

$$Nu_{DTTI} = 0.033199 Re_f^{0.800351} \mathrm{Pr}_f^{0.358743} (0.01 + P_d Y)^{-0.19756}. \tag{25}$$

Now Overall heat transfer coefficient (UA) of the HX is evaluated as,

$$\frac{1}{UA} = \frac{1}{\eta_o h_a A_a} + \frac{1}{h_f A_f} + \frac{\ln(\frac{d_0}{d_i})}{2\pi L \alpha_t} \frac{1}{UA} = \frac{1}{\eta_0 h_0 A_0} + \frac{1}{h_x A_i} + R_w. \tag{26}$$

Where overall surface effectiveness is determined as [60],

$$\eta_o = 1 - \frac{A_{fin}}{A_a} (1 - \eta_{fin}). \tag{27}$$

While the Effectiveness of cross unmixed fluid flow type HX is determined as [61],

$$\varepsilon = 1 - \exp \left[\frac{NTU^{0.22}}{C^*} \exp \left(-C^* NTU^{0.78} - 1 \right) \right]. \tag{28}$$

Where, $NTU = \frac{UA}{C_{\min}}$ and Net Heat transfer rate across HX is evaluated as,

$$Q = \varepsilon C_{\min} \left(T_{f,i} - T_{a,i} \right) \tag{29}$$

Tube side pumping power, Fan and tube pumping efficiency has considered as 65%, is calculated by,

$$P_{pp} = \frac{\Delta p_f \times CFR}{\eta_p} \tag{30}$$

Airside net pressure drop is determined by [62],

$$\Delta p_a = \frac{M V_a^2}{2\rho_{a,i}} \left[(1 + \sigma^2) \left(\frac{\rho_{a,i}}{\rho_{a,e}} - 1 \right) + f_a \frac{2F_d}{D_{h,a}} \left(\frac{\rho_{a,i}}{\rho_{a,e}} + 1 \right) \right]. \tag{31}$$

Fan power required to drive the fan has determined as,

$$F_P = \frac{A_{fr} \times V_a \times \Delta p_a}{\eta_p} \tag{32}$$

After evaluation of heat transfer and power consumption, a related performance parameter index has been evaluated as [63],

$$PI = \frac{Q}{P_{PP} + F_P}. \tag{33}$$

Second law analysis of wavy fin and tube air heat exchanger is necessary for qualitative energy analysis. Two unmixed fluid flow mainly air and hot fluid although air is considered as a compressible fluid flow while the latter one remains incompressible within the heat exchanger. Thus entropy generation is determined as the sum of airside entropy and tube side entropy. Net entropy generation is calculated as [26]:

$$\dot{S}_{gen} = \dot{m}_a\left[c_{p,a}\ln\frac{T_{a,e}}{T_{a,i}} - R_a\ln\frac{p_{a,e}}{p_{a,i}}\right] + \dot{m}_f\left[c_{p,hnf}\ln\frac{T_{f,e}}{T_{f,i}} - \frac{p_{a,e}-p_{a,i}}{\rho_{hnf}T_{f,mean}}\right]. \quad (34)$$

Exergy loss by hot fluid (Tube side) is the addition of heat transfer with thermal entropy generation and viscous entropy generation across tube side, is calculated as[27],

$$\Delta Ex_f = Q + T_0\left[\dot{m}_f c_{p,hnf}\ln\left(T_{f,i}/T_{f,e}\right) - \dot{m}_f\Delta p_f/(\rho_{hnf}T_{f,mean})\right]. \quad (35)$$

Whereas, cold air takes heat from the hotter fluid and exergy gain of air is evaluated as,

$$\Delta Ex_a = Q - T_0\left[\dot{m}_a c_{pa}\ln(T_{a,e}/T_{a,i}) + \dot{m}_a R\ln\left(p_{a,i}/p_{a,e}\right)\right]. \quad (36)$$

After exergy analysis of air and hotter fluid, Second law efficiency or Exergy efficiency is calculated as,

$$\eta_2 = \frac{\Delta Ex_a}{\Delta Ex_f} \quad (37)$$

Now, the irreversibility is given by,

$$I = T_0\dot{S}_{gen}. \quad (38)$$

Entropy generation Number, a Non-dimensional parameter adopted by Mishra et al. [64] to study the effect of heat capacity with entropy generation, is determined as,

$$N_{gen} = \frac{\dot{S}_{gen}}{C_{\max}}. \quad (39)$$

To identify ultimate utilization of the resources on application Sustainability index (SI) has been studied which is defined by the exergy ratio [65].

$$SI = \frac{1}{(1-\eta_2)}. \quad (40)$$

Based on different turbulators used in the investigation, the heat transfer enhancement coefficient has been defined as the Nusselt number ratio. It indicates the heat enhancement due to geometry modification. For different turbulators heat transfer enhancement compared to Nusselt number with plain tube define as,

$$Nu_r = \frac{(Nu_f)_{TTI/PTTI/DTTI}}{(Nu_f)_{PY}} \quad (41)$$

Due to the use of different turbulators, heat enhancement occurs at the cost of pressure drop penalty, relative pressure drop penalty coefficients for different inserts is defined as,

$$f_r = \frac{(f_f)_{TTI/PTTI/DTTI}}{(f_f)_{PT}} \quad (42)$$

The performance evaluation criteria (PEC) combines both heat transfer enhancement coefficient as well as relative pressure drop coefficient ratios to determine heat transfer improvement at a given pumping power consumption. To judge the practical luxury of Turbulator inserts in air HX, PEC was evaluated at equal power consumption. The mathematical formulation of pressure drop and coolant flow rate at constant power requirement for plain tube HX and turbulator inserts HX can be expressed as:-

$$(CFR\times\Delta p)_{PT} = (CFR\times\Delta p)_{TTI/PTTI/DTTI} \quad (43)$$

Further, it may be encountered as,

$$(f_f Re^3)_{PT} = (f_f Re^3)_{TTI/PTTI/DTTI} \quad (44)$$

On combining the equation (43) and (44), at a given pumping power PEC is defined by Webb et al. [66] as,

$$PEC = \frac{Nu_r}{(f_r)^{\left(\frac{1}{3}\right)}} \quad (45)$$

The utilization of various inserts and THNFs in heat exchangers enhances performance at cost of pumping power. Power consumption in terms of CO_2 discharge will be a major criterion for analysis. Coal-based power generation supplies electricity to the main power substation. CO_2 discharge analysis can be claimed to utilize carbon emission factors. CO_2discharge [67] evaluated as:

$$Dis_{CO_2} = \frac{f_{CO_2}P_{Net}t_{run}}{10^6} \quad (46)$$

Where $Dis_{CO_2}$is the carbon dioxide discharge to the environment in tons per year, f_{CO_2} represents the carbon discharge factor. The carbon discharge factor is taken to be 0.820 kgCO_2/kWh (Location based). P_{net}, represents the net power consumption in kW requires to run the equipment in an hour while t_{run} is the annual operating time (h/Annum) of the heat exchanger. Heat exchanger operating cost is determined by net electricity consumption and evaluated as [45]:

$$HX_{Operating\text{Cost}} = P_{Net}t_{run}C_{electricity} \quad (47)$$

Data analysis has been evaluated by assuming that Heat exchangers run continuously twenty-four working hours per day and a total of 180 days of the year before maintenance. The Electricity price ($C_{Electricity}$) has been considered as 8 per kWh.

2.4. Numerical procedure and model validation

The governing set of coupled equations has been solved using EES (Engineering Equation Solver) to evaluate the bulk mean temperature of both fluids, internal fluid (Hot fluid), and external fluid flow (air) for different Reynolds number. Estimation of temperature outlets is programmed to determine fluid properties. For four E's analysis of air heat exchanger with Turbulators for various THNFs, simulation methodology with the help of flow chart layout in the chronological order for the outcomes has been demonstrated in Fig. 3.

The stepwise numerical chronology of the present investigation for the outcomeare described below:

Step 1:Fluids entrance temperatures (T_{fi} = 70 °C, T_{ai} = 30 °C), Reynolds number, and THNF thermophysical properties at 0.6% volume fraction with constant air velocity 5 m/s have been assigned as an initial inlet condition for TTI inserts to air HX and simulated for particular THNF.

Step 2: EEES numerical simulated to determinethe convection heat transfer coefficient for air and THNF's for twisted turbulator inserts using a suitableset of correlations [57-61].

Step 3: Simulation is done to determine the air side, hot fluid side pressure drop, and heat transfer coefficient for the selected inserts and THNF.

Step 4: Overall heat transfer coefficient and pumping power is determined from the simulated code of EES.

Step 5: Using the $\mathcal{E}$-NTU technique, simulation is done to get the outlet temperatures of both fluids. A similar procedure is followed for PT, PTTI, and DTTI for different THNF properties at inlet conditions using the required correlations for inserts [27,43,44,55,56].Outcomes data are recorded for analysis and repeated the numerical procedure from step 1 for each Turbulator inserts using all six THNF's.

To check the validation of theoretical results, Simulated code results have been compared with the available experimental results [68] of HX. To compare from experimental results alumina water fluid has been air velocity set as a variable parameter. The entrance temperature of alumina water is 80 °C, the same air entry temperature has been considered, alumina water outlet temperatures and heat transfer rate effects with air velocity has been compared. It is found that a likewise trend of hot fluid outlet temperatures and heat transfer rate compared to experimental results shown in Fig. 4. Meanwhile, heat transfer rate differs maximum by 5% with the experimental data while 4% maximum difference found compared to experimental results in case of hot fluid outlet temperature. Comparison is based on a plain tube air heat exchanger using a nanofluid.

3. Result and discussion

Effects of TTI, PTTI, and DTTI on Nusselt number with Reynolds number of THNF6 utilized in air HX compared to the absence of turbulators are presented in Fig. 5. In general, the Nusselt number varies linearly with the Reynolds number. Linear variation is mainly due to amplified turbulent intensity, which is also a reason for intensified convective heat transfer coefficient. Turbulators used in air HX enhance the Nusselt number significantly. Although, turbulators created a radial intense mixing of the fluid which is normally absent in air HX without turbulators. The reason for the enhancement of Nusselt number in presence of turbulators in air HX is mainly due to swirl flow generation, thermal boundary layer interruption, and radial pressure gradient generation. However, among turbulators, PTTI and DTTI in HX shown the largest enhancement due to additional boundary layer interruption in presence of perforated and dimpled holes than TTI. Also larger the number of dimpled and perforated holes higher the Nusselt number in returns due to more and rapid interruption in the thermal boundary layer. Although, at lower Re (below 7900), due to increased resident time of fluid flow causes a higher percentage increment of nusselt number. However, TTI has shown 182.2 – 34.8%. PTTI has 214.2 – 46.2% while DTTI has 273.6 – 78.5% higher Nusselt number compared to HX without any turbulators at lowest and highest Reynolds number. Although, Friction loss caused due to the presence of with and without turbulators with Reynolds number in the range of (2400–15000) is presented in Fig. 5. Curve trends show a similar reduction of frictional loss of turbulators inserts and the plain tube. However, the friction factor shows a progressive decrement with an increased Reynolds number. At lower Re, high frictional forces occurred at the backward of twisted turbulators and thus enhance the vortices generation resulted in higher friction loss. The friction factor of turbulators is higher compared to plain tubes for obvious reasons. Mainly increased surface area in presence of turbulators, amplified swirl intensity, and the loss of higher viscosity vicinity to the tube surface and thus resulted in a blockage in fluid flow are several reasons for frictional factor loss. Although, TTI 63.6 – 66.4%, PTTI 164.7 – 186%, and DTTI resulted in 185 – 214.1% higher frictional factor compared to plain tube air HX.

Comparative effects of overall heat transfer coefficient and pressure drop across the HX of different turbulators for

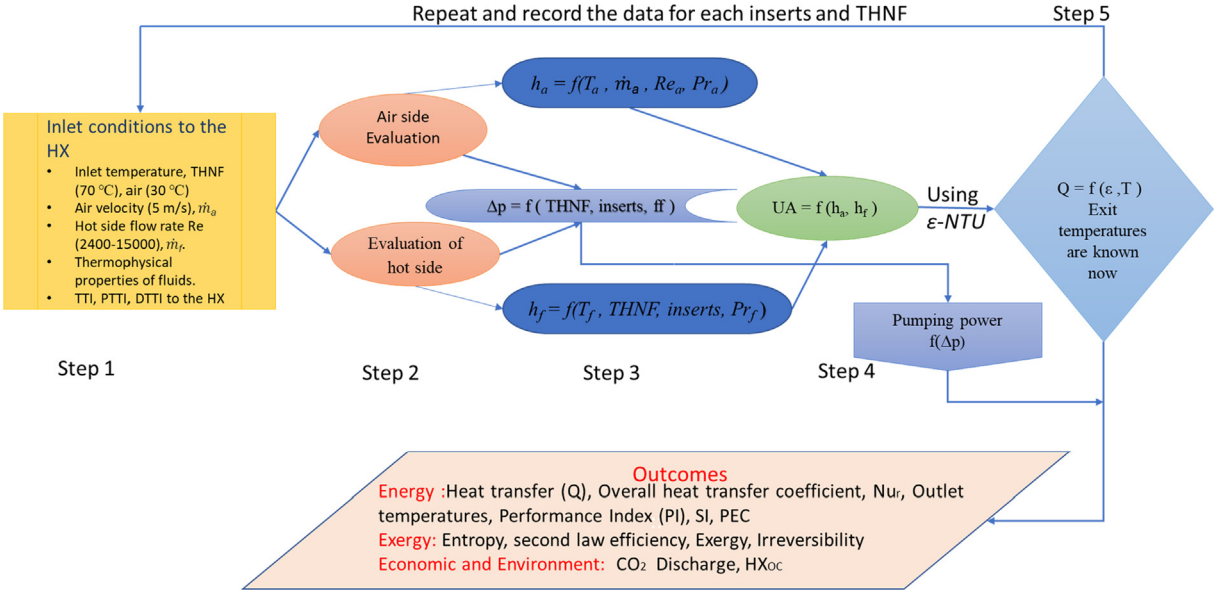

Fig. 3 Flow chart layout of the numerical procedure.

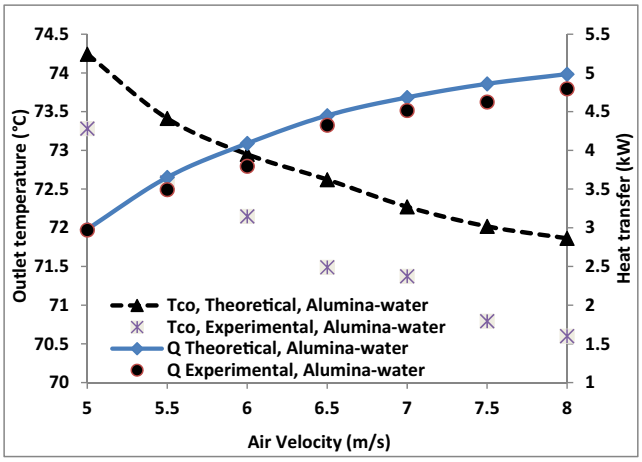

Fig. 4 Comparison of simulated results with experimental results [68].

THNF 6 (Al_2O_3 + Graphene + MWCNT-Water) with Reynolds number compared to plain tube has shown in Fig. 6 Turbulators cause swirl flow generation and a relative centrifugal force created between the turbulators and tube wall. Also, fluid residence time along with an increased mixed fluid flow between tube surface and tube core area amplifies the secondary flow therefore in turbulators overall heat transfer coefficient is higher compared to the plain tube for each Reynolds number. Now, among turbulators, DTTI has shown the highest overall heat transfer coefficient compared to PTTI while lowest for TTI. While at a lower Reynolds number, below 7900, a significant enhancement in presence of turbulators was found. At Re 3600, DTTI has 11%, PTTI has 8.9%, and TTI has7.7% higher overall heat transfer coefficient compared to without inserts in air HX. This could be due to DTTI and PTTI promoted the strength of swirl flow and regeneration of boundary layer near the dimpled and perforated area. Significant enhancement occurs with a penalty in pressure drop. Pressure drop variation with Reynolds number for various inserts for THNF has represented in Fig. 6. Pressure drop variation trend for turbulators found similar to the plain tube with Reynold number. Pressure drop increases with increased Reynolds number. Turbulators have resulted in higher pressure drops than the plain tube. Turbulators cause immense secondary flow, addition causes a high blockage of the fluid inside the tube of the tube with inserts and with high loss of viscosity which resulted in a higher pressure drop. Moreover, at lower Re, the pressure drop is lower while at higher Re, greater than 7900, causes an immense pressure drop could be due to higher interaction among pressure force and inertial force at the boundary layer. For THNF 6, DTTI has 190 – 214% higher pressure drop, PTTI has 169 – 185% higher penalty while TTI has 65 – 69% higher pressure drop penalty relative to without any inserts to air HX at lowest and highest Reynolds number respectively.

Nusselt number enhancement was found to be higher at a lower Reynolds number. This is because the impact of twisted turbulators was more dominant at lower Reynolds number while friction factor was more in low Reynolds number while relatively gets lower when mass flow rates increased. However, the heat transfer enhancement coefficient (Nu_r) as stated in equation (40) for various geometrical modifications of an air HX operated with several THNFs at 3600 Re is presented in Fig. 7. Air HX of DTTI showed the highest Nu_r and lowest was obtained in case of TTI while intermediate Nu_r for PTTI HX compared to smooth tube air HX. As TTI causes secondary flow near the twisted tape and increased the residing time of fluid flow while along with the above phenomenon perforated twisted turbulator additionally causes an interruption in the boundary layer near the perforated holes and dimpled curvature of DTTI produces additional strength to the swirl flow intensity and redevelopment of boundary layer generation of same hole diameter and pitch than PTTI which could be the reason for increased heat transfer enhancement ratio than

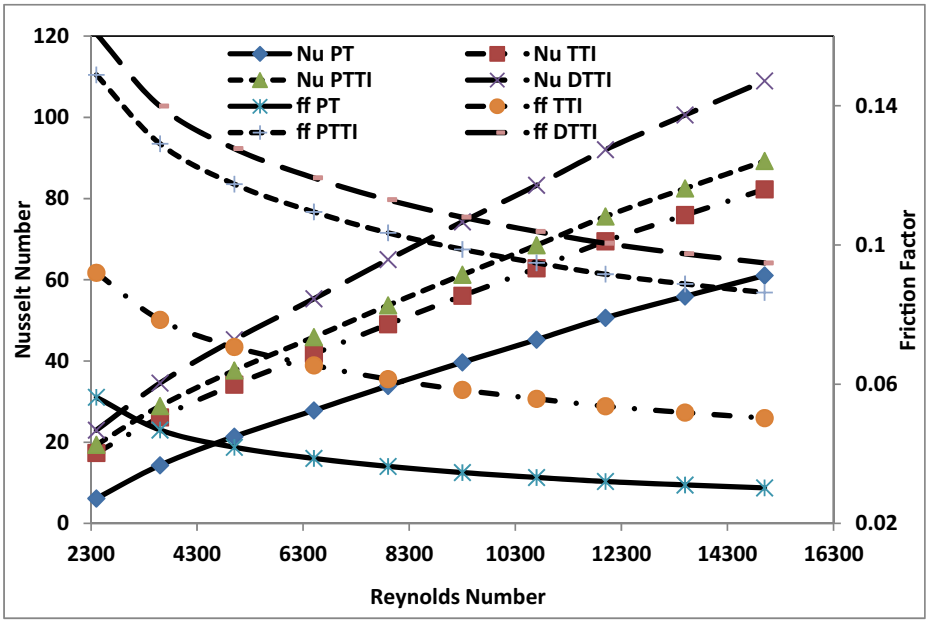

Fig. 5 Nusselt Number and Friction factor with Reynolds Number.

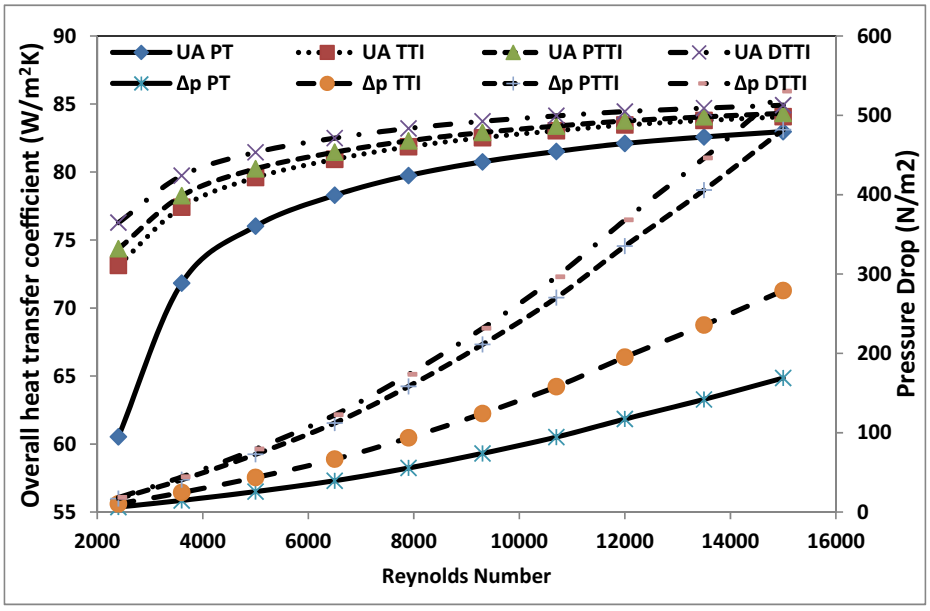

Fig. 6 Pressure drop and overall heat transfer coefficient with Reynolds number.

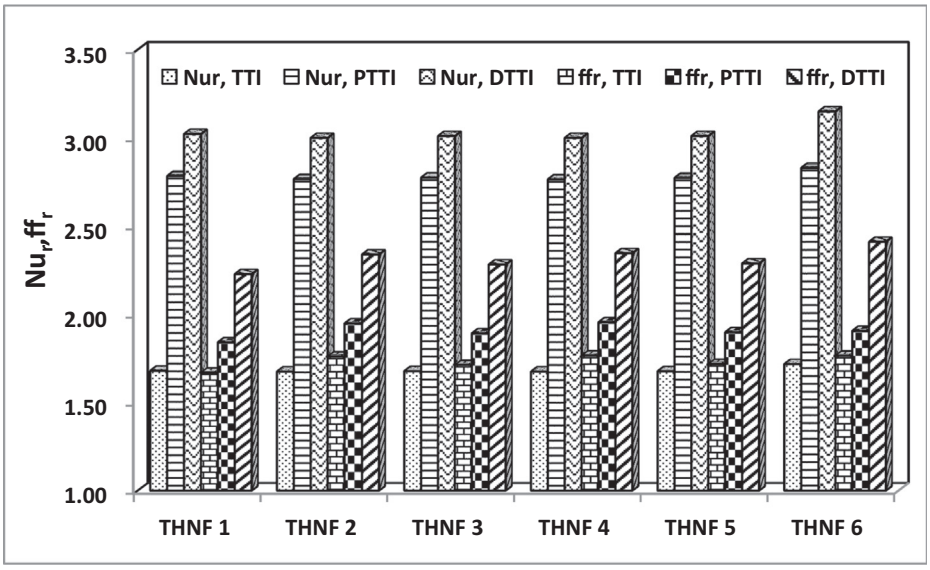

Fig. 7 Nusselt ratio and friction factor ratio with THNFs for various Turbulators.

smooth tube air HX. As per the Nusselt number enhancement ratio, working fluid THNF 6 should be preferred in the air HX. Furthermore, friction factor ratio (f_r) variation for different working fluids and under various turbulators is also shown in Fig. 6. Among Turbulators, DTTI has shown higher friction factor ratio than PTTI while the lowest is obtained in the case of TTI. DTTI caused strong flow vortices which further strengthen the swirl action compared to PTTI and TTI. This could be the motivation for the selection of turbulators at low Re. Moreover, as per the friction factor ratio, lower f_r should be preferred, therefore, THNF 1 (Al_2O_3 + CuO + TiO_2 -Water) and THNF 3 (Al_2O_3 + CuO + MWCNT-Water) should be preferred as working fluid in air HX for lower power consumption.

Performance evaluation criteria or thermal performance factor which identifies the practical use and benefits of the air HX with various turbulator inserts. PEC was evaluated to estimate the energy utilized in presence of various turbulators at a given input power using equation (44). Thermal performance factor variation with different turbulator inserts (TTI, PTTI, and DTTI) for different hot working fluids is presented in Fig. 8, Re 3600. For all the cases studied PEC more than unity is considered as an energy-saving in terms of performance enhancement. DTTI in air HX attributed the highest PEC for all hybrid nanofluid considered and showed a mean of 2.29 PEC. The lowest mean PEC of 1.40 was obtained in the case of TTI While PTTI in air HX contributed an intermediate mean PEC of 2.24. This is due to at lower Re, thermal

enhancement was more dominant compared to friction factor in presence of Turbulators. Moreover, Inspection of various hybrid working fluids utilizes in HX with various inserts reveals a little but significant variation in PEC. Among several THNFs, THNF 6 (Al_2O_3 + Graphene + MWCNT - Water) achieved the highest PEC than the rest of the hybrid working fluid studied. The preferred order of hybrid working fluid based on higher PEC in terms of energy savings would be THNF 6 most likely preferable while the least preferred hybrid nanofluid would be THNF 4 (Al_2O_3 + TiO_2 + Graphene–Water) therefore, for exergy, entropy, and second law analysis THNF 6 (Al_2O_3 + Graphene + MWCNT - Water) as a working fluid has been investigated.

Requirement of second law analysis in detail to have the minimum entropy and mean entropy principles within HX. The utilization of qualitative energy in terms of exergy change of coolant and exergy change in the air of an air HX under different geometrical modifications for THNF 6 at different Reynolds numbers is presented in Fig. 9. At lower Re, thermal entropy generation is dominant, both exergy change in air and exergy change in the coolant (hot fluid transfers energy to secondary fluid air) shows a large improvement with turbulators inserts, as inserts in the plain tube cause a restriction in flow and cause blockage of flow which amplifies the residence time which causes higher exergy exchange between the fluids compared to air HX of plain tube configuration. Also, the radial direction of fluid flow in turbulators causes further intensification in exergy exchange. Beyond Re 6500, however, an enhancement in exergy exchange continued due to increment in turbulent intensification although the rate of increment remains lower due to viscous entropy generation dominancy than thermal entropy. Although DTTI in air HX caused the highest (21.94 – 2.2%) exergy change of coolant due to high secondary flow generation than PTTI (19.4 – 1.5%) and lowest for TTI (17.7 – 1.2%) compared to air HX of plain tube configuration at lowest Re 2400 and highest Re 15,000 respectively. Due to a similar reason, exergy change of air was found highest in the case of DTTI at mean improvement of 9.65% and lowest for TTI with a mean enhancement of 6.6% compared to air HX of Plain tube configuration, while an intermediate range of enhancement found for PTTI air HX.

As the overall heat transfer coefficient in the case of air HX with DTTI was higher while lowest for air HX without turbulator inserts for the same reason, heat transfer has also shown similar variation with Reynolds number as shown in Fig. 10. At lower Re 2400, enhancement in heat transfer was found to be highest. Also, another dimensionless number entropy generation number variation with Reynolds number for various turbulator inserts is shown in Fig. 10. Entropy generation number depends upon the entropy generation and heat capacity. Increased Re increases the viscous entropy generation as well as thermal entropy generation of the fluids, although, higher Reynolds number viscous entropy generation dominates over thermal entropy generation. Thus, the entropy generation number increased with Re. However, a comparison analysis reveals that at Re 6500, DTTI has 4.9 %, PTTI 3.8 %, and TTI has a 3.2 % relatively higher entropy generation number compared to an air HX with plain tubes. Entropy generation number increment comparatively still lesser compared to Nusselt number enhancement of HX with various inserts therefore results suggest a better design of compact HX achieved with turbulators.

Effects of various six THNFs used as a working fluid on second law efficiency in air HX with different turbulator inserts at lower Re 3600 is explored in Fig. 11. Second law efficiency or exergetic efficiency indicates the utilization of qualitative energy to brings up better thermal design systems. Higher efficiency conveys an improved thermal design of the air HX. Although, different turbulators made a significant improvement in exergetic efficiency compared to air HX with plain tubes and it is due to a larger increase in exergy loss by the hot fluid (THNFs) than exergy gain in air. However, among turbulators, DTTI in air HX in any working fluid studied, showing the highest second law efficiency compared to remaining inserts while the lowest obtained for PT air HX. Thus, an air HX with various turbulators inserts effectively

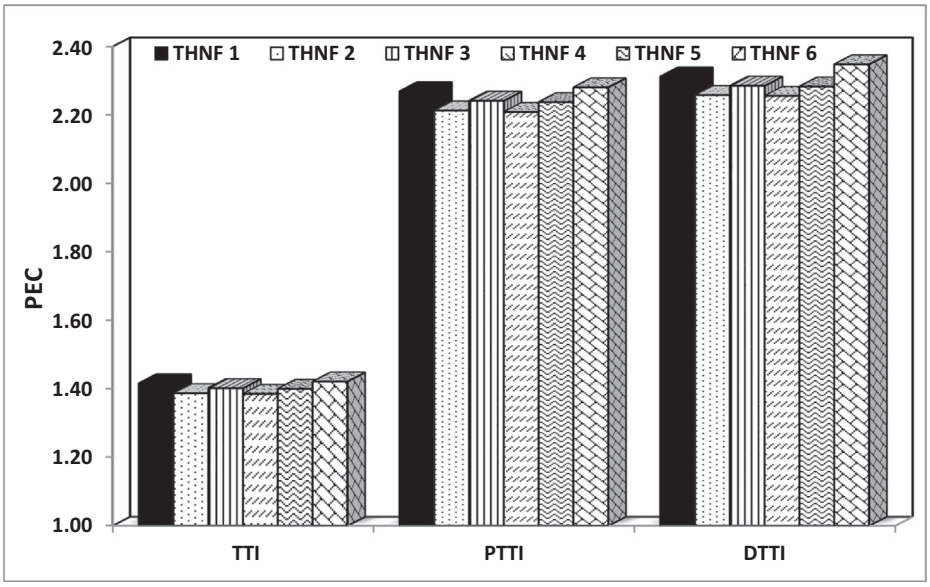

Fig. 8 PEC of Turbulators for THNFs.

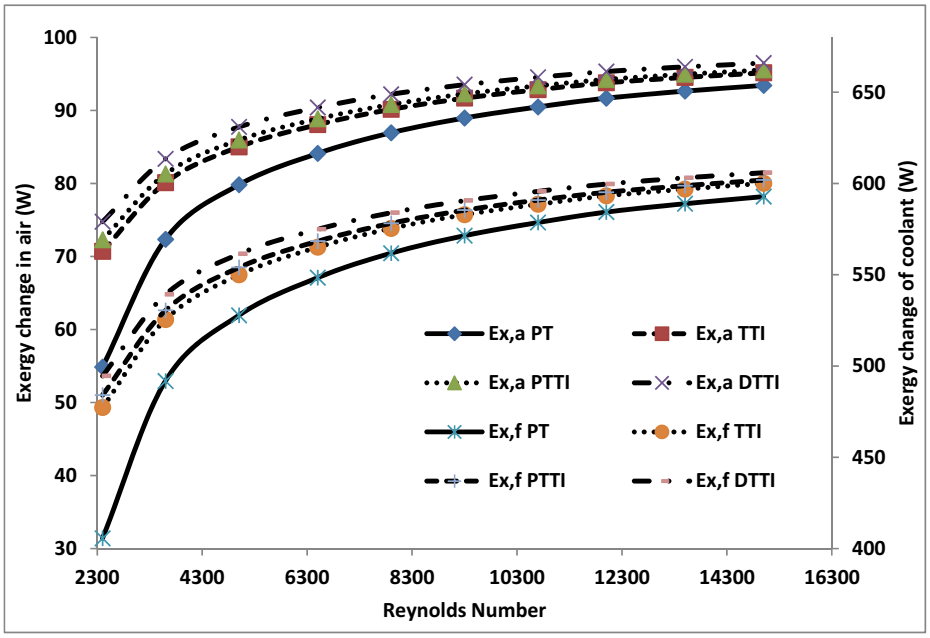

Fig. 9 Exergy change of coolant and air with Reynolds Number.

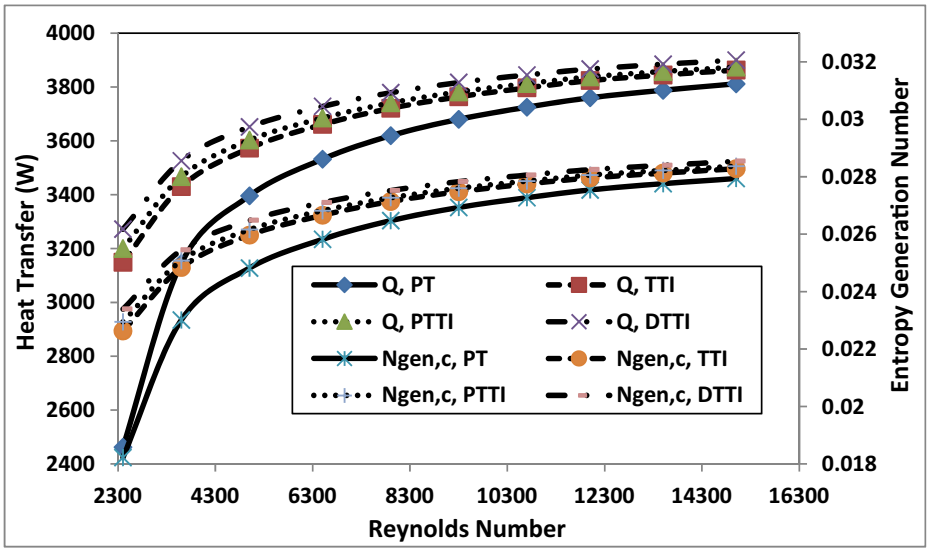

Fig. 10 Heat transfer and entropy generation number with Reynolds number.

aimed at a better thermal device. Although, THNF has also shown an impact on exergetic efficiency, the lowest percentage enhancement in the range of 1.54 – 2.54% of second law efficiency obtained for the THNF 1 (Al_2O_3 + CuO + TiO_2 - water) type for TTI and DTTI in air HX respectively while highest improvement in exergetic efficiency obtained when operated with THNF 6 (Al_2O_3 + Graphene + MWCNT-water) in the range of 1.9 – 2.84% for air HX with TTI and DTTI respectively compared to air HX with Plain tube configuration.Therefore from the second law analysis, and air HX operated with THNF 6 working fluid and DTTI turbulators performs better compared to other turbulators. However, for every turbulators studied, the preferred order of using THNF as a working fluid in air HX on exergetic efficiency basis to be as THNF 6 > THNF 4 > THNF 2 > THNF 5 > THNF 3 > THNF 1.

Also, a parameter that involves the combined effect of heat transfer, and power requirement to run an HX is the Performance index. The performance index of air HX under different geometrical modifications and various hybrid nanofluids is presented in Fig. 12 at Re 3600. DTTI offers higher swirl generation as well as boundary layer interruption due to the presence of dimpled on twisted turbulators which enhances heat transfer more compared to PTTI and TTI air HX than pumping power required. Therefore, the Performance index obtained highest when DTTI air HX has been used while among turbulators lowest obtained when air HX with PTTI and TTI is used. DTTI in air HX operated with different

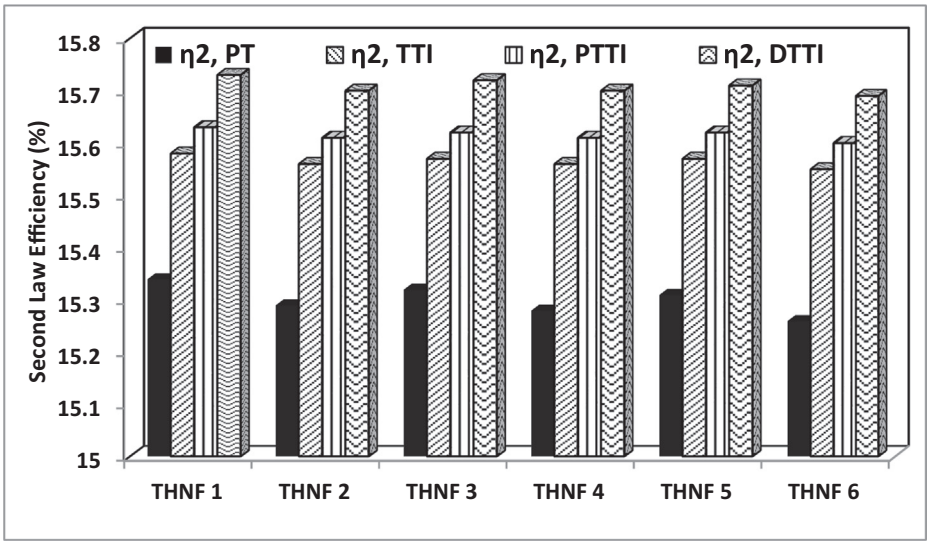

Fig. 11 Second law efficiency variation with turbulators utilizing THNFs.

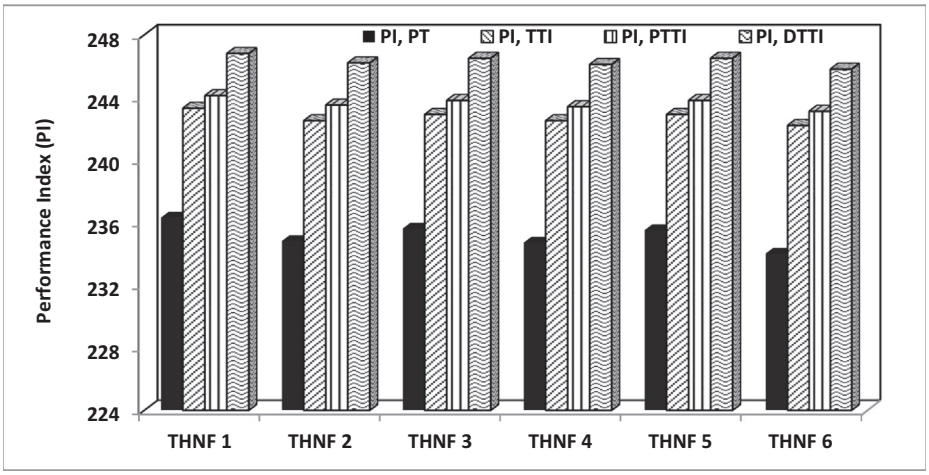

Fig. 12 Performance Index with THNFs for Turbulators.

THNF working fluid and found that DTTI has shown the lowest increment of 4.4% PI compared to air HX of plain tubes operated with THNF1(Al_2O_3 + CuO + TiO_2 -water) and highest PI improvement of 5 % when operated with THNF 6 (Al_2O_3 + Graphene + MWCNT-water) due to significant thermophysical behavior and morphological change. Among various hybrid nanofluid operated, a range of 2.9 – 3.5 % higher performance index obtained in TTI arrangement compared to plain tube air HX for THNF 1 and THNF 6 respectively. However different geometrical modifications operated with different hybrid nanofluid has shown a significant improvement in performance index and the order of performance index enhancement could be used as the selection of working fluid priority as THNF 6 > THNF 4 > THNF 2 > THNF 5 > THNF 3 > THNF 1 in any turbulators of an air HX compared to plain tube HX.

Moreover, the purpose of turbulators was to enhance the heat exchange between hot fluids (THNFs) or coolant and air in an HX. Various inserts enable Hotter fluid or coolant to transfer its heat to the air at a faster rate. So far now Lower Reynolds number shows a great improvement in heat transfer utilizing Turbulator inserts. Therefore, the coolant or hot fluid (THNF 6) outlet temperature of HX with various Turbulator inserts at lower Re (below 7900) is depicted in Fig. 13. When mass flow increased residence time decreased therefore temperature drop has reduced. However, turbulator inserts improved the radial fluid flow direction which allows the tube core hot fluid to strike on the tube wall from which air takes the heat. And due to the high radial temperature gradient, a higher temperature drop is possible. Although at Re 2400, DTTI has able to maximum of 1.05 °C, PTTI has 0.84 °C and TTI has managed to 0.74 °C lowered coolant temperature compared to air HX with plain tubes.

The best way to study energy utilization can be understood in terms of entropy analysis. Higher the entropy lesser effective use of energy within an HX. In general, thermodynamically, HX of lower entropy should be preferred. For a fluid flow, heat exchange process, entropy causes due to thermal change as well as the pressure drop across the flow. As seen from Fig. 14, thermal change is quite appreciable in low Reynolds

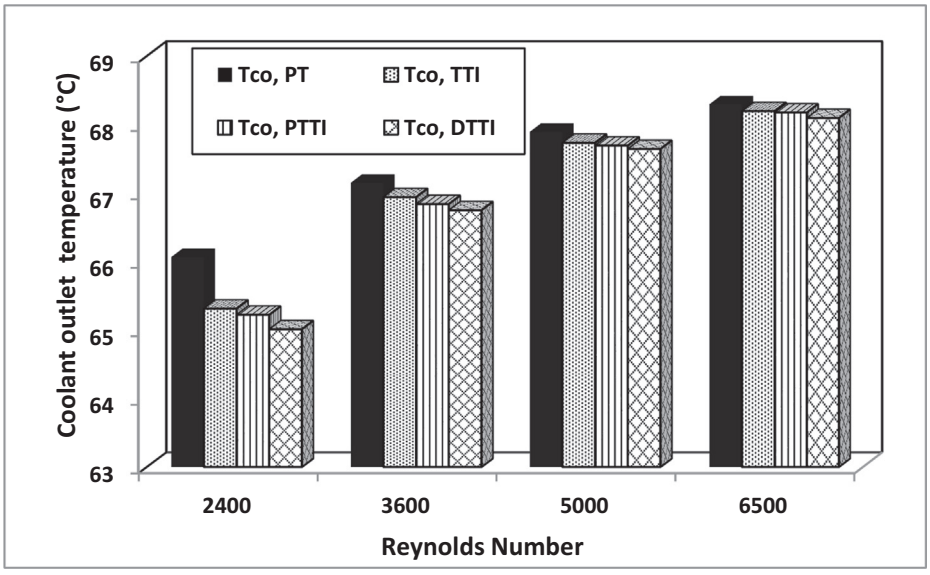

Fig. 13 Coolant outlet temperature with Reynolds Number.

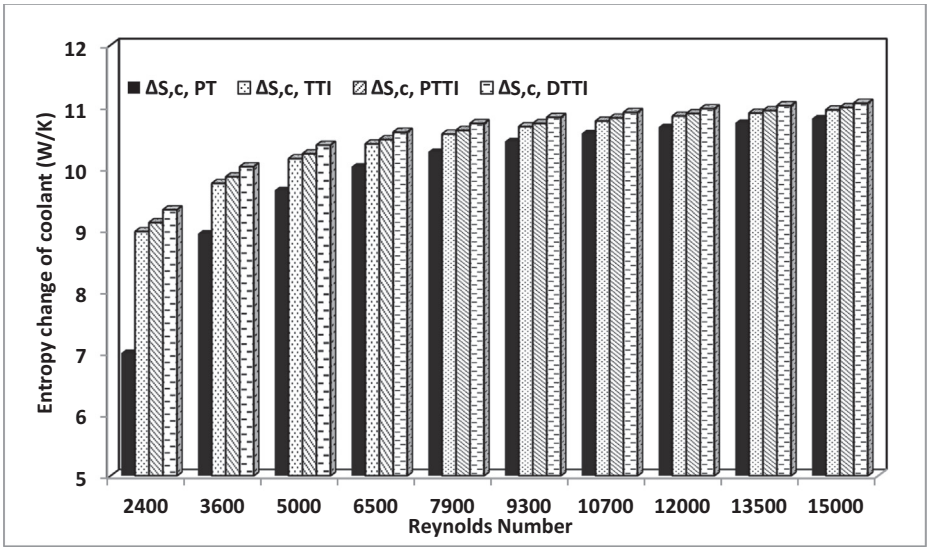

Fig. 14 Entropy change of coolant with Reynolds Number for various Turbulators.

number and beyond that mass flow rate increment thermal change is little significant and viscous entropy gets dominant. Therefore, the entropy change of coolant remains near about the same, see Fig. 14, beyond Re 6500. Although, among studied turbulators, the highest entropy change of 5.6 % in the case of DTTI, 4.4 % intermediate for PTTI, and lowest 3.7 % for TTI air HX compared to without turbulated air HX at Re 6500. Also, Irreversibility variation with Re for different Turbulators in HX for THNF 6 as a working fluid is presented in Fig. 15. Irreversibility signifies the entropy generation as it is proportional to it while, entropy generation is proportional to the mass flow rate therefore, the trend shows increased irreversibility with Re.

Irreversibility also signifies the exergy loss difference among heat exchanging fluids [36]. It is found that even turbulators inserts cause higher irreversibility compared to without Turbulator insert. A common order of higher heat transfer and pressure drop follows as DTTI showed highest and lowest for TTI while an intermediate variation in PTTI air HX of studied working fluids. This is due to DTTI creates extra vorticity and produces a regeneration of boundary layer at the dimpled positions and is sufficiently more than that has produced at perforated positions. Moreover, a comparison analysis reveals that at Re 6500, DTTI turbulators inserts have caused 4.2 %, followed by PTTI 3.1% and 2.5% least higher irreversible TTI air HX compared to that of without inserts air HX.

A non-dimensional parameter, SI, depends upon coolant exergy change and exergy loss, which reveals the effective energy utilization. However, a study reveals that SI increased with the increase in the mass flow rate of coolant. A variation in SI with several studied working fluids for different turbulator inserts of air HX is presented in Fig. 16. Air HX without

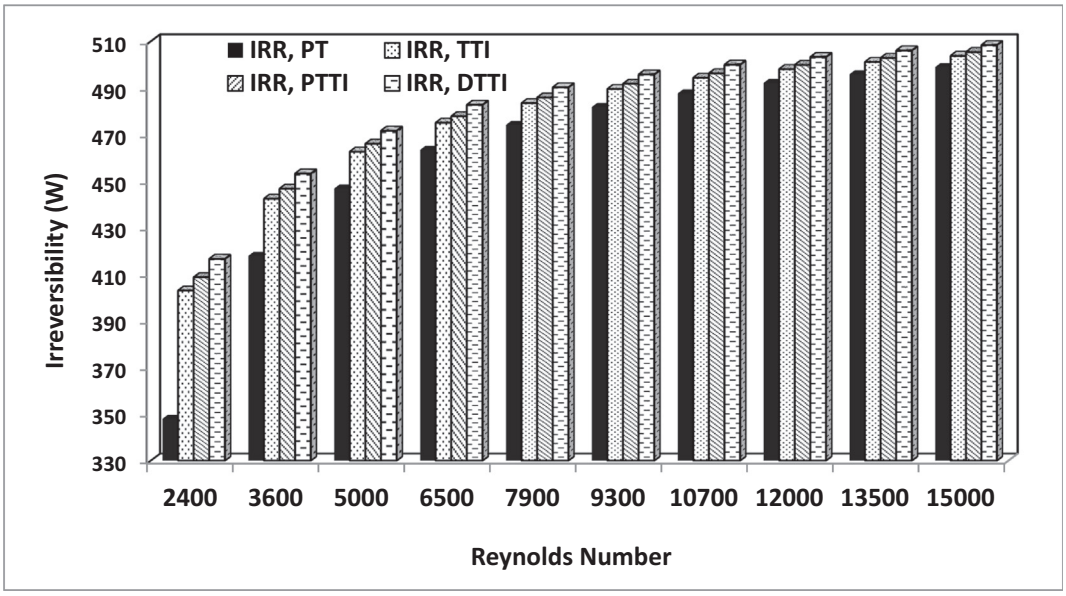

Fig. 15 Irreversibility with Reynolds Number for various Turbulators.

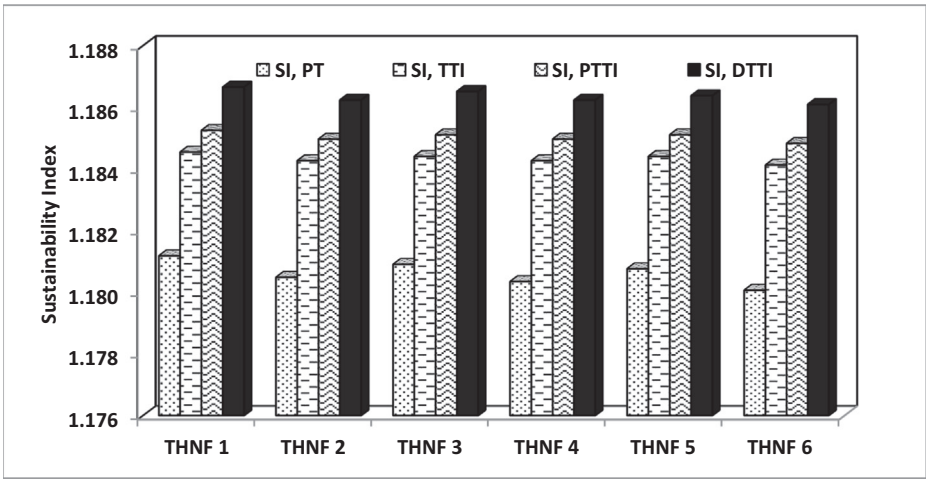

Fig. 16 Sustainability Index of various THNFs with Turbulators.

inserts shows relatively lower SI compared to inserts. Meanwhile, As coolant exergy change is highest in the case of DTTI. Thus, DTTI resulted to be a genuine higher SI for all working fluid cases studied among different turbulators investigated. DTTI showed a maximum SI of 1.187 numerical value when working fluid is THNF 1. Although comparing increment in SI with PT air HX from other tube inserts for the different working fluid, then THNF 6 has maximum enhancement. So on the basis of SI in terms of percentage enhancement, different tube inserts, compared to PT air HX order of preferred working fluid as a coolant is THNF 6 (Al_2O_3 + Graphene + MWCNT - Water) > THNF 4 (Al_2O_3 + TiO_2 + - Graphene -Water) > THNF 2 (Al_2O_3 + CuO + Graphene - Water) > THNF 5 (Al_2O_3 + TiO_2 + MWCNT - Water) > THNF 3 (Al_2O_3 + CuO + MWCNT - Water) > THNF 1 (Al_2O_3 + CuO + TiO_2 - Water). Therefore, hybrid nanofluids of different shapes are most likely to have the highest enhancement relative to like morphology.

Power supply to the air HX for pumping power of pump and fan to run continuously requires coal combustion, therefore, discharge of CO_2 annually and HX operating cost for various operating fluids of different Tube inserts in a compact air HX is shown in Fig. 17. HX operated for 180 days caused the highest CO_2 discharge required of 10.4 kg for DTTI air HX while a minimum 5.2 kg requirement of CO_2 discharge is obtained without inserts air HX. Also, related HX operating cost investigated which shows a similar trend of variation discharge CO_2 discharge varied with THNFs and various inserts. While TTI requires 30.5 %, PTTI 80 %, and DTTI 90.8% higher average CO_2 discharge compared to without inserts HX. Among investigated THNFs, compared to plain tube HX, for different tube inserts, a lesser operating cost would

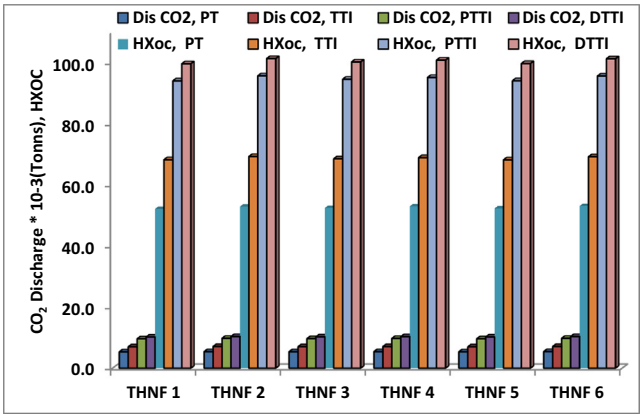

Fig. 17 CO_2 Discharge and HX OC with THNFs for various Turbulators.

be preferable as THNF 4 > THNF 5 > THNF 6 > THNF 3 > THNF 1 > THNF 2. The operating cost of THNF 2 is highest due to a larger pressure drop compared to other hybrid nanofluids investigated. Therefore, where lower cost is a requirement THNF 4 should be selected as a working fluid in air HX with inserts.

4. Conclusion

In this present investigation, compact air heat exchanger device with various performance improvement technique is studied. Air passed through HX to takes heat from the coolant or hot fluid. Tripartite hybrid water-based nanofluids are used as hot fluid instead of simple water. Different Turbulator (TTI, PTTI, and DTTI) inserts are introduced in air HX and compared performance parametersto the PT air HX. Effect on performance parameters with Reynolds number and THNFs are also studied. Modified turbulator inserts are compared on energy, exergy, irreversibility, entropy, exergo-economic, sustainability, and environmental aspects. The following key points are:

- Tripartite hybrid nanofluid utilized in air HX shows mild improvement, while THNFs with modified turbulator inserts in air HX provide remarkable enhancement, as DTTI turbulator shows highest 183% and 111.3% Nu_r compared to TTI and PTTI respectively using THNF 6 working fluid.
- The highest overall heat transfer coefficient obtained for DTTI air HX using THNF 6, at Re 2400 with a 26% net improvement than PT air HX.
- The highest PEC in turbulators are obtained for THNF 6 in DTTI air HX, 4% higher PEC than THNF 4 working fluid.
- Cost analysis and carbon discharge to the environment reveal THNF 2 to be least and THNF 4 to be most likely preferred working fluid as THNF 2 working fluid requires91.4% higher running cost than PT air HX.
- The DTTI modified turbulators with THNF6 as a working fluid shows the best choice to be used as working fluid due to higher overall heat transfer coefficient, 21.94% exergy change, 2.94 %second law efficiency, 5.04% performance index and 0.5% higher sustainable index than without inserts air HX.
- At lowest Re 2400, DTTI shows highest 33.12% Coolant entropy change, 19.73% irreversibility, and 28.3% entropy generation number, than PT air HX followed by PTTI, and TTI using THNF 6 working fluid.

Declaration of Competing Interest

The authors declare that they have no known competing financial interests or personal relationships that could have appeared to influence the work reported in this paper.

Acknowledgement

None.

References

[1] S. Liu, M. Sakr, A comprehensive review on passive heat transfer enhancements in pipe exchangers, Renew. Sustain. Energy Rev. 1 (19) (2013 Mar) 64–81.
[2] Y. Lei, F. Zheng, C. Song, Y. Lyu, Improving the thermal hydraulic performance of a circular tube by using punched delta-winglet vortex generators, Int. J. Heat Mass Transf. 1 (111) (2017 Aug) 299–311.
[3] M.T. Naik, S.S. Fahad, L.S. Sundar, M.K. Singh, Comparative study on thermal performance of twisted tape and wire coil inserts in turbulent flow using CuO/water nanofluid, Exp. Therm Fluid Sci. 1 (57) (2014 Sep) 65–76.
[4] S. Ponnada, T. Subrahmanyam, S.V. Naidu, A comparative study on the thermal performance of water in a circular tube with twisted tapes, perforated twisted tapes and perforated twisted tapes with alternate axis, Int. J. Therm. Sci. 1 (136) (2019 Feb) 530–538.
[5] H. Bucak, F. Yilmaz, The current state on the thermal performance of twisted tapes: a geometrical categorisation approach, Chem. Eng. Process.-Process Intensif. 29 (2020 May) 107929.
[6] S. Eiamsa-ard, P. Seemawute, K. Wongcharee, Influences of peripherally-cut twisted tape insert on heat transfer and thermal performance characteristics in laminar and turbulent tube flows, Exp. Therm Fluid Sci. 34 (6) (2010 Sep 1) 711–719.
[7] P. Murugesan, K. Mayilsamy, S. Suresh, P.S. Srinivasan, Heat transfer and pressure drop characteristics in a circular tube fitted with and without V-cut twisted tape insert, Int. Commun. Heat Mass Transfer 38 (3) (2011 Mar 1) 329–334.
[8] P. Murugesan, K. Mayilsamy, S. Suresh, Turbulent heat transfer and pressure drop in tube fitted with square-cut twisted tape, Chin. J. Chem. Eng. 18 (4) (2010 Aug 1) 609–617.
[9] P. Murugesan, K. Mayilsamy, S. Suresh, Heat transfer in tubes fitted with trapezoidal-cut and plain twisted tape inserts, Chem. Eng. Commun. 198 (7) (2011 Mar 2) 886–904.
[10] W.X. Chu, C.A. Tsai, B.H. Lee, K.Y. Cheng, C.C. Wang, Experimental investigation on heat transfer enhancement with twisted tape having various V-cut configurations, Appl. Therm. Eng. 25 (172) (2020 May) 115148.
[11] M.E. Nakhchi, M. Hatami, M. Rahmati, Experimental investigation of heat transfer enhancement of a heat exchanger tube equipped with double-cut twisted tapes, Appl. Therm. Eng. 5 (180) (2020 Nov) 115863.
[12] M.E. Nakhchi, J.A. Esfahani, Numerical investigation of rectangular-cut twisted tape insert on performance improvement of heat exchangers, Int. J. Therm. Sci. 1 (138) (2019 Apr) 75–83.
[13] A.R. Suri, A. Kumar, R. Maithani, Heat transfer enhancement of heat exchanger tube with multiple square perforated twisted tape inserts: experimental investigation and correlation

development, Chem. Eng. Process. Process Intensif. 1 (116) (2017 Jun) 76–96.
[14] K. Nanan, C. Thianpong, P. Promvonge, S. Eiamsa-Ard, Investigation of heat transfer enhancement by perforated helical twisted-tapes, Int. Commun. Heat Mass Transfer 1 (52) (2014 Mar) 106–112.
[15] C. Man, J. Yao, C. Wang, The experimental study on the heat transfer and friction factor characteristics in tube with a new kind of twisted tape insert, Int. Commun. Heat Mass Transfer 1 (75) (2016 Jul) 124–129.
[16] M.M. Bhuiya, M.S. Chowdhury, M. Saha, M.T. Islam, Heat transfer and friction factor characteristics in turbulent flow through a tube fitted with perforated twisted tape inserts, Int. Commun. Heat Mass Transfer 1 (46) (2013 Aug) 49–57.
[17] M. Khoshvaght-Aliabadi, M. Farsi, S.M. Hassani, N.H. Abu-Hamdeh, A. Alimoradi, Surface modification of transversely twisted-turbulator using perforations and winglets: An extended study, Int. Commun. Heat Mass Transfer 1 (120) (2021 Jan) 105020.
[18] S. Eiamsa-Ard, K. Wongcharee, P. Eiamsa-Ard, C. Thianpong, Heat transfer enhancement in a tube using delta-winglet twisted tape inserts, Appl. Therm. Eng. 30 (4) (2010 Mar 1) 310–318.
[19] S. Eiamsa-Ard, K. Wongcharee, P. Eiamsa-Ard, C. Thianpong, Thermohydraulic investigation of turbulent flow through a round tube equipped with twisted tapes consisting of centre wings and alternate-axes, Exp. Therm. Fluid Sci. 34 (8) (2010 Nov 1) 1151–1161.
[20] S.Y. Won, P.M. Ligrani, Flow characteristics along and above dimpled surfaces with three different dimple depths within a channel, J. Mech. Sci. Technol. 21 (11) (2007 Nov 1) 1901.
[21] M.A. Akhavan-Behabadi, R. Kumar, A. Mohammadpour, M. Jamali-Asthiani, Effect of twisted tape insert on heat transfer and pressure drop in horizontal evaporators for the flow of R-134a, Int. J. Refrig. 32 (5) (2009 Aug 1) 922–930.
[22] M. Moravej, M.V. Bozorg, Y. Guan, L.K. Li, M.H. Doranehgard, K. Hong, Q. Xiong, Enhancing the efficiency of a symmetric flat-plate solar collector via the use of rutile TiO2-water nanofluids, Sustain. Energy Technol. Assess. 1 (40) (2020 Aug) 100783.
[23] O.A. Hussein, K. Habib, A.S. Muhsan, R. Saidur, O.A. Alawi, T.K. Ibrahim, Thermal performance enhancement of a flat plate solar collector using hybrid nanofluid, Sol. Energy 1 (204) (2020 Jul) 208–222.
[24] M. Goodarzi, I. Tlili, Z. Tian, M.R. Safaei, Efficiency assessment of using graphene nanoplatelets-silver/water nanofluids in microchannel heat sinks with different cross-sections for electronics cooling, Int. J. Numer. Meth. Heat Fluid Flow (2019 Jun 22).
[25] T. Ambreen, A. Saleem, H.M. Ali, S.A. Shehzad, C.W. Park, Performance analysis of hybrid nanofluid in a heat sink equipped with sharp and streamlined micro pin-fins, Powder Technol. 1 (355) (2019 Oct) 552–563.
[26] V. Kumar, R.R. Sahoo, Exergy and energy performance for wavy fin radiator with a new coolant of various shape nanoparticle-based hybrid nanofluids, J. Therm. Anal. Calorim. 5 (2020 Feb) 1–2.
[27] R.R. Sahoo, V. Kumar, Impact of Novel Dissimilar Shape Ternary Composition-Based Hybrid Nanofluids on the Thermal Performance Analysis of Radiator, J. Therm. Sci. Eng. Appl. (2021). Aug 1;13(4).
[28] M. Sahu, J. Sarkar, Steady-state energetic and exergetic performances of single-phase natural circulation loop with hybrid nanofluids, J. Heat Transfer (2019). Aug 1;141(8).
[29] P. Kumam, T. Anwar, W. Watthayu, Z. Shah, Double Slip Effects and Heat Transfer Characteristics for Channel Transport of Engine Oil With Titanium and Aluminum Alloy Nanoparticles: A Fractional Study, IEEE Access 22 (9) (2021 Mar) 52036–52052.
[30] V. Kumar, R.R. Sahoo, Experimental And Numerical Study On Cooling System Waste Heat Recovery For Engine Air Preheating By Ternary Hybrid Nanofluid, J. Enhanced Heat Transfer. 28 (4) (2021).
[31] T. Anwar, P. Kumam, Z. Shah, K. Sitthithakerngkiet, Significance of Shape Factor in Heat Transfer Performance of Molybdenum-Disulfide Nanofluid in Multiple Flow Situations; A Comparative Fractional Study, Molecules 26 (12) (2021 Jan) 3711.
[32] T. Anwar, P. Kumam, P. Thounthong, K. Sitthithakerngkiet, Nanoparticles shape effects on thermal performance of Brinkman-type ferrofluid under heat injection/consumption and thermal radiation: A fractional model with non-singular kernel and non-uniform temperature and velocity conditions, J. Mol. Liq. 1 (335) (2021 Aug) 116107.
[33] T. Anwar, P. Kumam, I. Khan, W. Watthayu, Heat Transfer Enhancement in Unsteady MHD Natural Convective Flow of CNTs Oldroyd-B Nanofluid under Ramped Wall Velocity and Ramped Wall Temperature, Entropy. 22 (4) (2020 Apr) 401.
[34] T. Anwar, P. Kumam, P. Thounthong, Fractional Modeling and Exact Solutions to Analyze Thermal Performance of Fe 3 O 4-MoS 2-Water Hybrid Nanofluid Flow Over an Inclined Surface With Ramped Heating and Ramped Boundary Motion, IEEE Access 14 (9) (2021 Jan) 12389–12404.
[35] M. Sheikholeslami, S.A. Farshad, Z. Ebrahimpour, Z. Said, Recent progress on flat plate solar collectors and photovoltaic systems in the presence of nanofluid: a review, J. Cleaner Prod. 28 (2021 Jan) 126119.
[36] M. Sheikholeslami, M. Jafaryar, Z. Said, A.I. Alsabery, H. Babazadeh, A. Shafee, Modification for helical turbulator to augment heat transfer behavior of nanomaterial via numerical approach, Appl. Therm. Eng. 5 (182) (2021 Jan) 115935.
[37] A. Hasanpour, M. Farhadi, K. Sedighi, Intensification of heat exchangers performance by modified and optimized twisted tapes, Chem. Eng. Process.-Process Intensif. 1 (120) (2017 Oct) 276–285.
[38] E. Esmaeilzadeh, H. Almohammadi, A. Nokhosteen, A. Motezaker, A.N. Omrani, Study on heat transfer and friction factor characteristics of γ-Al2O3/water through circular tube with twisted tape inserts with different thicknesses, Int. J. Therm. Sci. 1 (82) (2014 Aug) 72–83.
[39] K.V. Sharma, L.S. Sundar, P.K. Sarma, Estimation of heat transfer coefficient and friction factor in the transition flow with low volume concentration of Al2O3 nanofluid flowing in a circular tube and with twisted tape insert, Int. Commun. Heat Mass Transfer 36 (5) (2009 May 1) 503–507.
[40] K.A. Hamid, W.H. Azmi, R. Mamat, K.V. Sharma, Heat transfer performance of TiO2–SiO2 nanofluids in a tube with wire coil inserts, Appl. Therm. Eng. 1 (152) (2019 Apr) 275–286.
[41] M.C. Reddy, V.V. Rao, Experimental investigation of heat transfer coefficient and friction factor of ethylene glycol water based TiO2 nanofluid in double pipe heat exchanger with and without helical coil inserts, Int. Commun. Heat Mass Transfer 1 (50) (2014 Jan) 68–76.
[42] M.E. Nakhchi, J.A. Esfahani, Cu-water nanofluid flow and heat transfer in a heat exchanger tube equipped with cross-cut twisted tape, Powder Technol. 1 (339) (2018 Nov) 985–994.
[43] R.R. Sahoo, V. Kumar, Development of a new correlation to determine the viscosity of ternary hybrid nanofluid, Int. Commun. Heat Mass Transfer 1 (111) (2020 Feb) 104451.
[44] R.R. Sahoo, Thermo-hydraulic characteristics of radiator with various shape nanoparticle-based ternary hybrid nanofluid, Powder Technol. 15 (370) (2020 Jun) 19–28.
[45] S. Kashyap, J. Sarkar, A. Kumar, Performance enhancement of regenerative evaporative cooler by surface alterations and using ternary hybrid nanofluids, Energy. 15 (225) (2021 Jun) 120199.

[46] R.R. Sahoo, Heat transfer and second law characteristics of radiator with dissimilar shape nanoparticle-based ternary hybrid nanofluid, J. Therm. Anal. Calorim. 22 (2020 Jul) 1–3.
[47] M. Bahiraei, S. Heshmatian, Efficacy of a novel liquid block working with a nanofluid containing graphene nanoplatelets decorated with silver nanoparticles compared with conventional CPU coolers, Appl. Therm. Eng. 25 (127) (2017 Dec) 1233–1245.
[48] M. Bahiraei, N. Mazaheri, F. Aliee, Second law analysis of a hybrid nanofluid in tubes equipped with double twisted tape inserts, Powder Technol. 1 (345) (2019 Mar) 692–703.
[49] S. Eiamsa-ard, K. Wongcharee, K. Kunnarak, M. Kumar, V. Chuwattabakul, Heat transfer enhancement of TiO 2-water nanofluid flow in dimpled tube with twisted tape insert, Heat Mass Transf. 55 (10) (2019 Oct) 2987–3001.
[50] S.K. Singh, J. Sarkar, Improving hydrothermal performance of double-tube heat exchanger with modified twisted tape inserts using hybrid nanofluid, J. Therm. Anal. Calorim. 5 (2020 Feb) 1–2.
[51] S. Heshmatian, M. Bahiraei, Numerical investigation of entropy generation to predict irreversibilities in nanofluid flow within a microchannel: effects of Brownian diffusion, shear rate and viscosity gradient, Chem. Eng. Sci. 23 (172) (2017 Nov) 52–65.
[52] M. Bahiraei, N. Mazaheri, A. Bakhti, Irreversibility characteristics of nanofluid flow under chaotic advection in a minichannel for different nanoparticle types, J. Taiwan Inst. Chem. Eng. 1 (88) (2018 Jul) 25–36.
[53] T. Tharayil, L.G. Asirvatham, M.J. Dau, S. Wongwises, Entropy generation analysis of a miniature loop heat pipe with graphene–water nanofluid: thermodynamics model and experimental study, Int. J. Heat Mass Transf. 1 (106) (2017 Mar) 407–421.
[54] C.C. Wang, W.L. Fu, C.T. Chang, Heat transfer and friction characteristics of typical wavy fin-and-tube heat exchangers, Exp. Therm Fluid Sci. 14 (2) (1997 Feb 1) 174–186.
[55] M. Sahu, J. Sarkar, L. Chandra, Transient thermo-hydraulics and performance characteristics of single-phase natural circulation loop using hybrid nanofluids, Int. Commun. Heat Mass Transfer 1 (110) (2020 Jan) 104433.
[56] E.V. Timofeeva, J.L. Routbort, D. Singh, Particle shape effects on thermophysical properties of alumina nanofluids, J. Appl. Phys. 106 (1) (2009 Jul 1) 014304.
[57] Gnielinski V, Forced convection ducts, in Heat Exchanger Design Handbook, Schlunder, E. U., Ed., Hemisphere, Washington, DC, 1983, 2.5.1–2.5.3.
[58] R.M. Manglik, A.E. Bergles, "Heat transfer and pressure drop correlations for twisted-tape inserts in isothermal tubes: Part II—transition and turbulent flows, J. Heat Transfer 115 (4) (1993) 890–896.
[59] E. Smithberg, F. Landis, Friction and forced convection heat-transfer characteristics in tubes with twisted tape swirl generators, J. Heat Transfer 86 (1) (1964) 39–48.
[60] T. Dagdevir, V. Ozceyhan, An experimental study on heat transfer enhancement and flow characteristics of a tube with plain, perforated and dimpled twisted tape inserts, Int. J. Therm. Sci. 159 (2021 Jan) 106564.
[61] K.A. Hamid, W.H. Azmi, M.F. Nabil, R. Mamat, Experimental investigation of nanoparticle mixture ratios on TiO2–SiO2 nanofluids heat transfer performance under turbulent flow, Int. J. Heat Mass Transf. 1 (118) (2018 Mar) 617–627.
[62] Z. Said, M.E. Assad, A.A. Hachicha, E. Bellos, M.A. Abdelkareem, D.Z. Alazaizeh, B.A. Yousef, Enhancing the performance of automotive radiators using nanofluids, Renew. Sustain. Energy Rev. 1 (112) (2019 Sep) 183–194.
[63] A. Khan, H.M. Ali, R. Nazir, R. Ali, A. Munir, B. Ahmad, Z. Ahmad, Experimental investigation of enhanced heat transfer of a car radiator using ZnO nanoparticles in H 2 O–ethylene glycol mixture, J. Therm. Anal. Calorim. 138 (5) (2019 Dec) 3007–3021.
[64] M. Mishra, P.K. Das, S. Sarangi, Second law basedoptimization of crossflow plate-fin heat exchanger design using genetic algorithm, Appl. Therm. Eng. 29 (15) (2009 Jul) 2983–2989.
[65] M.A. Rosen, I. Dincer, M. Kanoglu, Role of exergy in increasing efficiency and sustainability and reducing environmental impact, Energy policy. 36 (1) (2008 Jan 1) 128–137.
[66] R.L. Webb, Performance evaluation criteria for use of enhanced heat transfer surfaces in heat exchanger design, Int. J. Heat Mass Transf. 24 (4) (1981 Apr 1) 715–726.
[67] H. Caliskan, I. Dincer, A. Hepbasli, Exergoeconomic, enviroeconomic and sustainability analyses of a novel air cooler, Energy Build. 1 (55) (2012 Dec) 747–756.
[68] J. Albadr, S. Tayal, M. Alasadi, Heat transfer through heat exchanger using Al_2O_3 nanofluid at different concentrations, Case Stud. Therm. Eng. 1 (1) (2013 Oct 1) 38–44.